Sust. Build. **3**, 3 (2018)

https://doi.org/10.1051/sbuild/2018002

Sustainable Buildings

Available online at:
www.sustainable-buildings-journal.org

Topical issue on: Zero Energy Mass Custom Homes

RESEARCH ARTICLE OPEN ACCESS

Solar water heating systems for different buildings under a hot climate; parametric optimization and economic analysis

Kheira Tabet Aoul*, Ahmad Hasan, and Hassan Riaz

Architectural Engineering Department, College of Engineering, United Arab Emirates University, P.O. Box 15551 Al Ain, UAE

Received: 16 December 2017 / Accepted: 14 May 2018

Abstract. Building applied solar thermal systems are considered by different stakeholders an attractive alternative to traditional space and water heating systems. However, their performance depends largely on climatic conditions, water heating needs and operational parameters which, in turn, offer opportunities for performance optimization. The present research attempts to provide architects with a design decision tool that integrates solar thermal collectors efficiently to meet hot water demand for various building types inclusive of residential, commercial and industrial in a hot climate. The analysis is conducted numerically through a thermal model developed and executed in TRNSYS and validated experimentally. The parameters investigated include the collector tilt angle, azimuth angle and collector inlet fluid flow rate. Finally, the collector aperture area required per building foot print area is determined. The research revealed that for a 1000 m^2 footprint building area of schools, offices, residential, factories and hospitals would require respectively 8 m^2, 10 m^2, 14 m^2, 24 m^2 and 38 m^2 of the static collector installed at 24° tilt angle with optimal water flow rate. Additional operational aspects of collector tracking, and solar radiation concentration were investigated and further reduce the required collector area. A simple payback period analysis reveals a return on investment of 2 years applying subsidized tariff rates under the climatic conditions of, or similar to Dubai, in the United Arab Emirates.

Keywords: solar water heating systems / building applied / parametric optimization / hot climate / performance assessment

1 Introduction

Dubai, in the United Arab Emirates (UAE) increased its energy demand from 33 742 to 43 093 GWh between 2010 and 2016, while adding 2639 MW electrical power capacity in the same period from 7361 to 10 000 MW (Fig. 1) indicating a sharp surge in its energy demand [1]. The capacity addition presented here is solely from gas, oil fired power plants, and does not include renewables. The curve shows that until 2015, the traditional power plants were merely meeting the demand. Afterwards, the demand surpassed the supply. In terms of energy consumption, the commercial sector leads with 47.5% followed by residential buildings at 28.5% as illustrated in Figure 2 as of 2016 [1]. This substantial energy needed in buildings contributes to carbon dioxide emissions, heightening the global warming effect [2] that can merely be addressed by integrating sustainable means of energy supply. Out of the total energy consumed in buildings, space and water heating needs range from 81% in cold climates [3] to 30% in hot climates [4] which justifies investing into alternative heating solutions to reduce the environmental footprint. The immense solar radiation potential reported in the UAE with measured average daily insolation of 4.98 kWh/m^2 and peak intensity ranging between 900 and 1100 W/m^2 in different seasons [5,6,7]. These statistics offer a promising source of heat supply through solar systems to meet hot water demand in UAE with the appropriate system sizing and configurations.

The performance of solar-assisted heating and cooling (SHC) systems was compared to the conventional cooling system for two building configurations in the UAE to determine optimal share of solar thermal in the building energy mix. The findings suggest a maximum solar penetration of 20% that results in an energy and CO_2 savings of 176 kWh/year and 140 ton/year with a payback period of 4 years [8]. In another study, the solar thermal collector area and hot water tank volume were optimized for a solar powered absorption cycle under UAE's weather conditions. The findings reveal that a specific collector area of 6 m^2/kW_c and a specific tank volume of 0.1 m^3/kW_c offer an optimal design that reduced energy consumption by 47% and CO_2 emissions by 12 tons/year compared to a conventional vapor-compression cooling system [9]. These limited experimental studies conducted in the UAE

* e-mail: kheira.anissa@uaeu.ac.ae

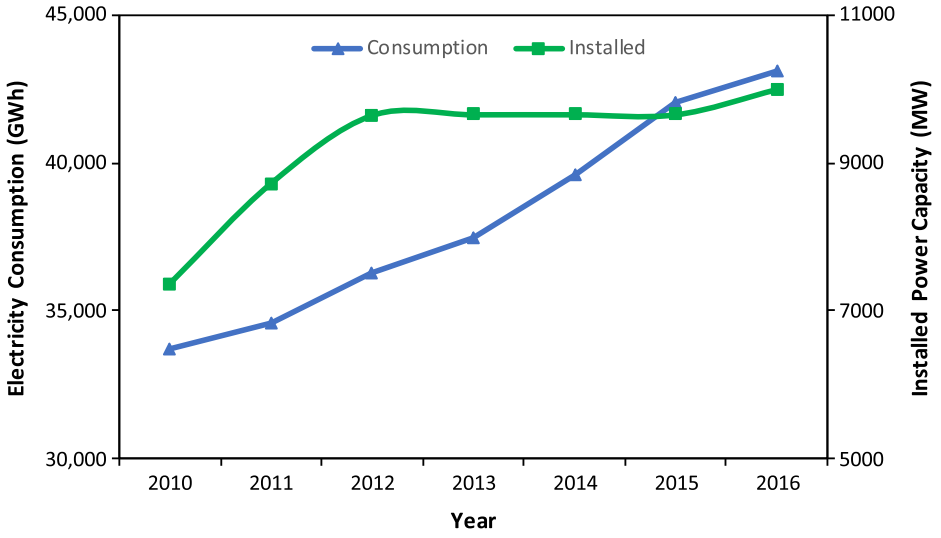

Fig. 1. Growth of electricity consumption and generation in Dubai, United Arab Emirates (UAE) [1].

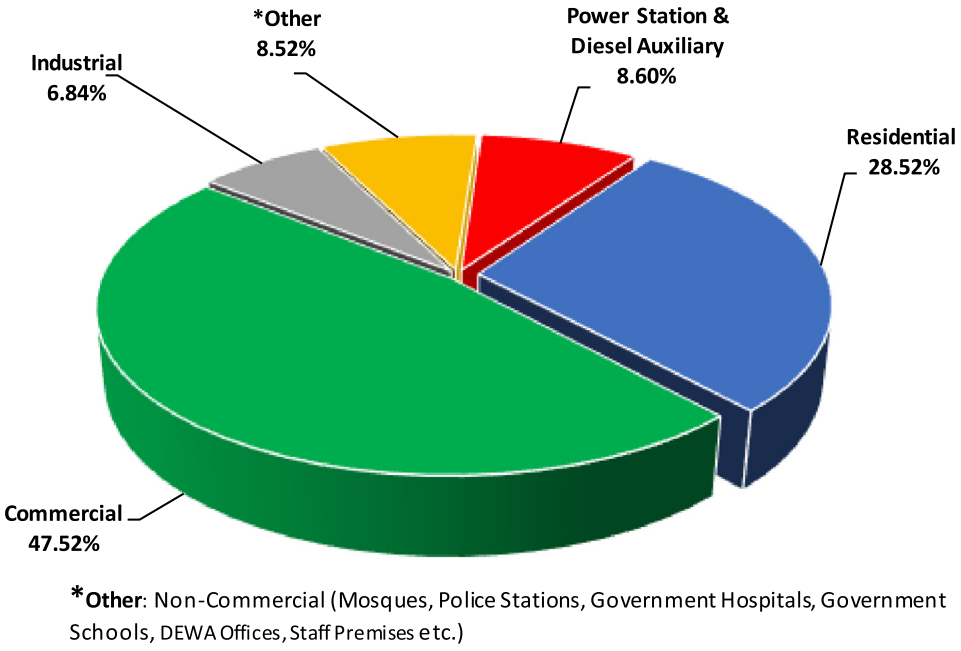

Fig. 2. Electricity consumption in different sectors of Dubai, United Arab Emirates (UAE) [1].

revealed that Solar Water Heating Systems (SWHS) are efficient and form an economically viable option to meet the hot water demand in buildings.

However, little is reported about optimal parameters that affect SHW performance inclusive of determining an optimal tilt angle (Φ) for the main UAE cities (Abu Dhabi and Dubai) [10,11]. This study considered the capital city, Abu Dhabi which lies at a latitude of $\varphi = 24°$. A detailed parametric optimization investigation is highly needed while considering various hot water demand patterns of different building typology. The current study attempts to numerically investigate collector parameters comprehensively to optimize the collector performance with regard to building types and hot water demands employing a TRNSYS thermal model [12]. The parameters considered include collector tilt angle, azimuth angle and collector inlet fluid flow rate. Additionally, the effect of inlet water temperature, collector tracking and solar radiation concentration were investigated. The objective of this study is to determine design parameters represented by the ratio of collector aperture area to building area for each of the studied building types while assessing its economic viability and system performance.

2 Methodology

The transient thermal model developed in TRNSYS is composed of a solar thermal collector and an auxiliary heating source. Simulations were carried out to assess the

Table 1. Hot water demand and water temperature per building type of a set area of 1000 m^2.

Parameters	Residential	Hospital	School	Office	Factories
Floor area allowance per occupant (square meter per person) [13]	19	Patient room: 11 Other spaces: 22	Classroom: 2 Vocational spaces: 5	9	9
Occupant load (Number of people)	53	68	350	111	111
Hot water demand (gallon per person per day) [14,15]	35	35	3	5	10
Total hot water demand per building use (gallon per day)	1855	2380	1050	555	1110
Water temperature Tr (°C) [13]	45	65	45	45	70–110

contribution and effectiveness of SWHS in meeting specific hot water demands in various building types. The building types considered include residential, schools, hospitals, offices and factories. For this investigation and comparison, all building types are considered to be 1000 m^2 in size. Buildings with spatially different occupant loads, such as hospitals and schools, have been considered accordingly, with half of the building area dedicated to each. The occupant load, water demand and required water temperature are calculated from relevant codes [13,14]. Table 1 summarizes the input data parameters.

2.1 Simulation model set up

The flat-plate solar collector is simulated using Hottel–Whillier steady-state model [16] which predicts the heat gain as a function of collector aperture area (A_c), number of identical collectors (n_c) and weather conditions as presented in equation (1);

$$Q_c = \frac{A_c}{n_c}\sum_{k=1}^{n_c} f_{r,k}[I_{ti}(\tau\alpha) - U_{c,k}(T_{i,k} - T_a)]. \quad (1)$$

The model employs overall energy gain efficiency factor (f_r,k), total incident solar radiation (I_{ti}), collective losses (U_c,k), temperature of fluid entering the collector (T_i) and ambient temperature (T_a) to calculate collector heat gain (Q_c). The f_r,k is an exponential function of the collector aperture area and thermal capacity (C_{pc}) as given in equation (2);

$$f_{r,k} = \frac{n_c m_c c_{pc}}{A_c U_{c,k}}\left(1 - e^{-\frac{f_c U_{c,k} A_c}{n_c m_c c_{pc}}}\right). \quad (2)$$

The product of transmittance and absorptance of the collector absorber plate for beam radiation $(\tau\alpha)_b$, diffused-radiation $(\tau\alpha)_d$, and ground reflectance $(\tau\alpha)_g$ are calculated by the trigonometric co-relation considering collector relative position to the incoming solar radiation given in equation (3);

$$\tau\alpha = \frac{I_b(\tau\alpha)_b + I_d\left(\frac{1+\cos\beta}{2}\right)(\tau\alpha)_d + r_g I_t\left(\frac{1-\cos\beta}{2}\right)(\tau\alpha)_g}{I_T}. \quad (3)$$

(U_c,k) is overall loss-coefficient by Klein composed of radiation and convection from top and bottom collector surfaces [16]. These losses are a function of number of glass covers (n_g), collector fin efficiency (f_c), number of collectors (n_c), Stefan Boltzmann's constant (σ), emissivity of glass cover (ϵ_g), absorber plate emittance (ϵ_p) and loss coefficients for edges and bottom (U_{be}) as depicted in equation (4).

$$U_{c,k} = \frac{3.6}{n_g}\left\{\left[\frac{c}{T_{p,k}}\left(\frac{T_{av,k-T_a}}{n_g + f}\right)\right]^{0.33} + \frac{1}{h_w}\right\} + \frac{3.6\sigma(T_{av,k}^2 + T_a^2)(T_{av,k} + T_a)}{\frac{1}{\varepsilon_p + 0.05 n_g(1-\varepsilon_p)} + \frac{2n_g + f - 1}{\varepsilon_g} n_g} + U_{be}. \quad (4)$$

The stratified thermal storage tank with variable inlets conditions is employed having an immersed coiled heat exchanger, with five segments for thermal lamination. The temperatures of hot water tank at the outer side (T_{hw2}) and average temperature at inner side (T_{hwa}) were calculated by using equations (5) and (6) [17].

$$\frac{dT_{\text{tank}}}{dt} = \frac{Q_{\text{in,tank}} - Q_{\text{out,tank}}}{c_{\text{tank}}}, \quad (5)$$

$$\frac{dT_{HX}}{dt} = \frac{Q_{\text{in},HX} - Q_{\text{out},HX}}{c_{HX}}, \quad (6)$$

where $Q_{\text{in,tank}}$ and $Q_{\text{out,tank}}$ depend on heat exchanger temperature, ambient temperature and solar irradiation. The $Q_{\text{in,HX}}$ and $Q_{\text{out,HX}}$ depend on inlet fluid temperature and tank temperature. The temperatures T_{hw2} and T_{hwa} are calculated by opting equations (7) and (8).

$$T_{hw2} = \left(T_{hw1} + \frac{b_{\text{ave}}}{a}\right)e^{a\Delta t} - \frac{b_{\text{ave}}}{a}, \quad (7)$$

$$T_{hwa} = \frac{1}{a\Delta t}\left(T_{hw1} + \frac{b_{\text{ave}}}{a}\right)(e^{a\Delta t} - 1) - \frac{b_{\text{ave}}}{a}, \quad (8)$$

where a and b are the coefficients of the differential equation in the form $dT/dt = aT + b$ and $b_{\text{ave}} = bT_{\text{ave}}$.

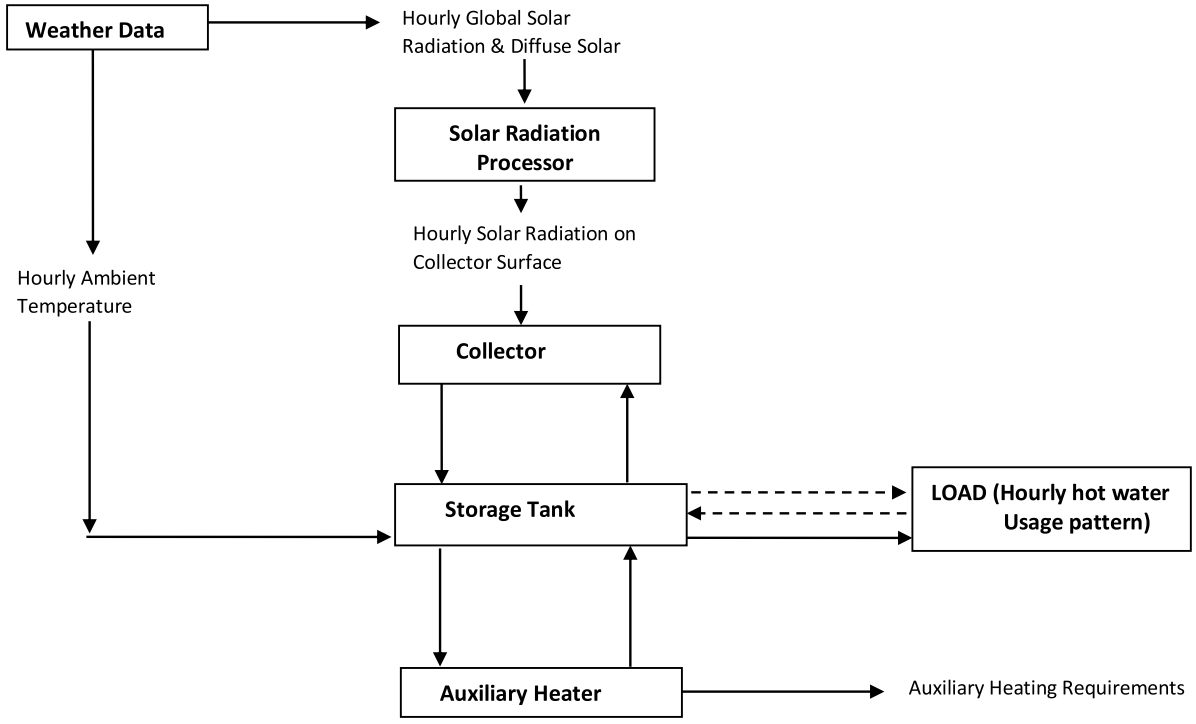

Fig. 3. Information flow diagram of micro-simulation for SWHS [19].

Figure 3 shows the information flow diagram for the micro-simulation of solar water heating and Figure 4 shows the flow diagram of TRNSYS for SWHS. The components of the SWHS considered are flat plate solar collector, water pump, storage tank and auxiliary electric heater. The system comprises of a 2 m^2 flat-plate collector with 1HP water pump and 325 gallons of water tank. A simulation model predicted the long-term thermal performance of the FPC.

The literature findings show that solar collector efficiency varies from 40 to 60% [18] as a function of inlet and ambient conditions as shown in Figure 5 [19]. The inputs for simulation include hot water usage pattern, system specifications and weather data. The time resolved weather data of interest is processed in "weather" block to feed into the thermal model represented by "collector". A feedback ON-OFF control loop is in place between the collector outlet and demand side temperature (T_{tank}) shown by the "controller" block to trigger water through collector by sensing tank temperature and availability of resource (solar radiation).

2.2 Building typology

The building typology is defined by hot water use pattern and set point temperatures in the present study. In literature, several standard hot water usage patterns are reported for the US and Europe [20,21], while very little is available on the subject for hot weather as of UAE. The pattern shown in Figure 6 is used to estimate a standard demand for residential, hospital and office buildings [22–24] in the UAE. In the current simulations, the end use temperature is set at 45 °C for residential, school and office buildings and 65 °C for hospital buildings.

3 Results and discussion

The thermal model developed in TRNSYS is validated with experimental data measured from a flat plate collector installed at the same site. Simulations are conducted employing typical means year (TMY-2) weather data for Abu Dhabi. The collector operational parameters of tilt angle, heat transfer fluid flow rate and heat loss coefficients are set in the TRNSYS model representing the experimental set up and ambient conditions. Temperatures were measured at front surface and leaving water from the collector and compared with the model prediction as shown in Figure 7. The results show a reasonable agreement between experimental and simulated temperatures with deviation of less than 5% at the most. The validated model is used to predict effects of collector operational parameters on the energy produced from the collector presented in the following sections.

3.1 Collector tilt angle

The performance of solar collector depends on its inclination angle [25,26]. Designers generally locate collectors on the building roof (pitched or flat) or on the façade (vertical wall). The same is simulated by varying monthly collector tilt angle (Φ) from 0° (representing flat roof) to 90° (representing south facing façade) with an increment of 5° representing various roof pitch angles while keeping at 0° azimuth representative of a south facing collector in the northern hemisphere. The average thermal gain (Q_c) is plotted against Φ as shown in Figure 8 to determine the optimal Φ for each month. The Q_c for January (winter) was 1.95 (kWh/m^2) at Φ of 0° which

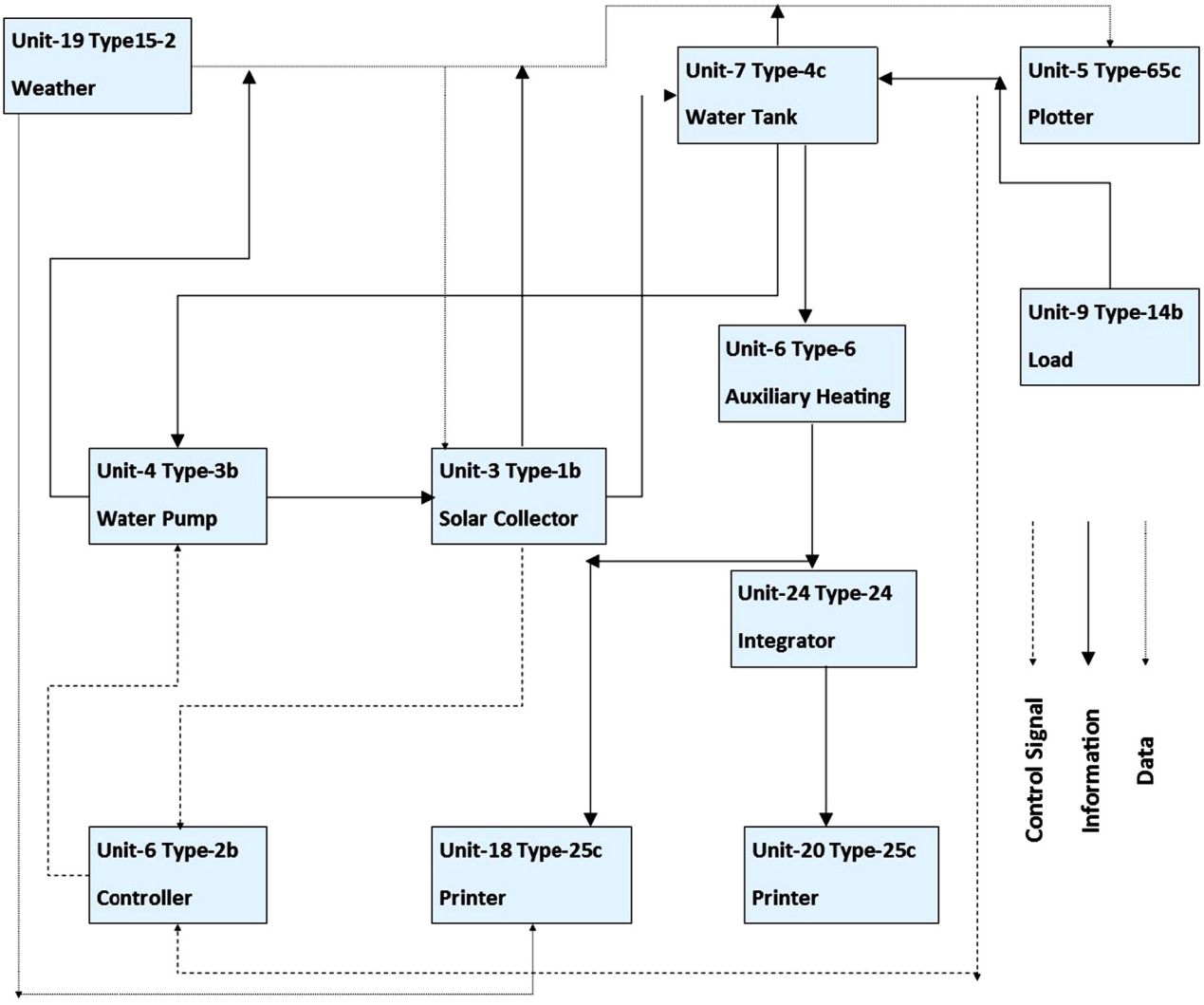

Fig. 4. Information flow diagram of TRNSYS for SWHS.

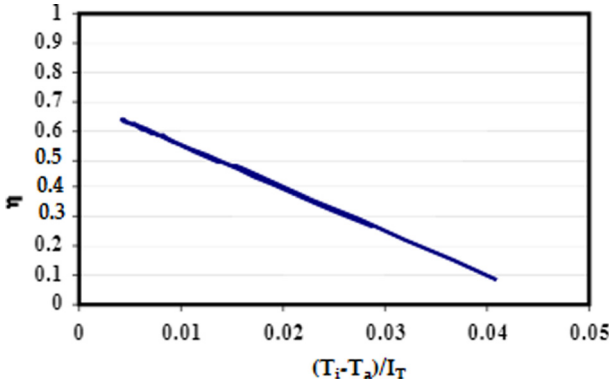

Fig. 5. Solar collector efficiency curve [19].

kept increasing to reach at 3.25 (kWh/m^2) at Φ of 50° (pitched roof). Beyond 50°, it kept dropping to reach to 2.2 (kWh/m^2) at Φ of 90° (vertical wall). It can be deduced that 50° is the optimal pitch angle for south-facing collector in January for Abu Dhabi. Similarly, for summer months i.e. May, the average Q_c was 4.11 (kWh/m^2) at Φ of 0° which kept decreasing with increasing Φ to reach 0.75 (kWh/m^2) at 90°, suggesting that 0° is the optimal Φ in May. Similarly, the optimal Φ for each month was determined based on maximal Q_c presented in Table 2.

To determine the yearly optimal fixed pitch angle, the collector slope was varied from 12 to 36° to simulate the off-latitude collector performance by up to ±12°. The maximum yearly Q_c of 1207.47 (kWh/m^2) was obtained at 24°, the latitude of the place as shown in Figure 9, which agrees with previous findings [27]. The findings highlight that the collector performance can greatly be optimized by monthly adjustment of Φ instead of yearly fixed value with little to no additional cost while bringing substantial benefits.

The architects may encounter design-dictated situations to install collectors either as wall mounted (for high rise buildings) or roof installed (sloped or flat). Hence, knowing the compromise between the design preferences and the prospective energy production would be informative. Thus, the yearly thermal performance of the collector installed at a sloped roof of (24°), flat roof (0°) and vertical

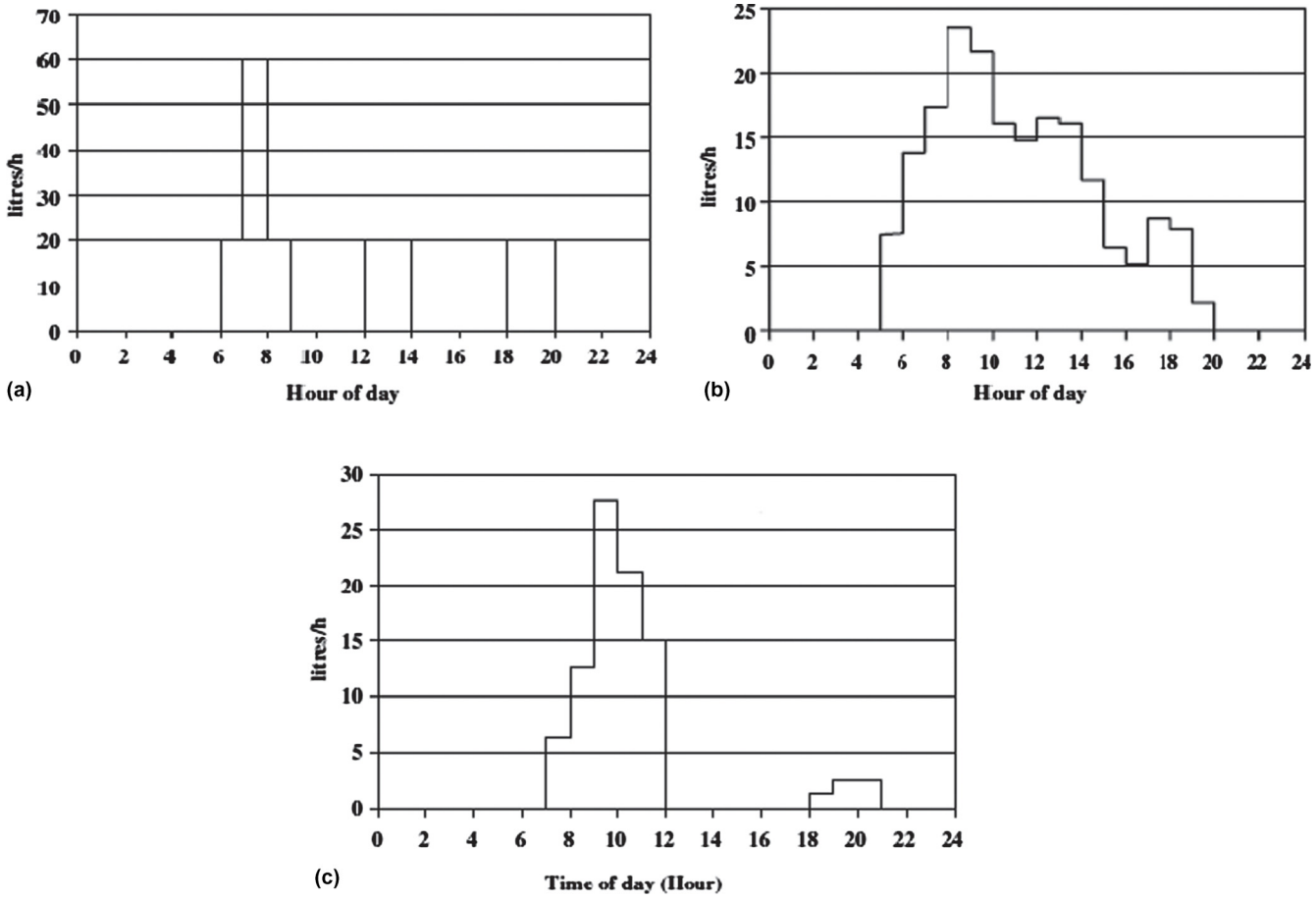

Fig. 6. Hot water usage pattern for (a) residential (b) hospital (c) office [22–24] under the hot weather conditions as of UAE.

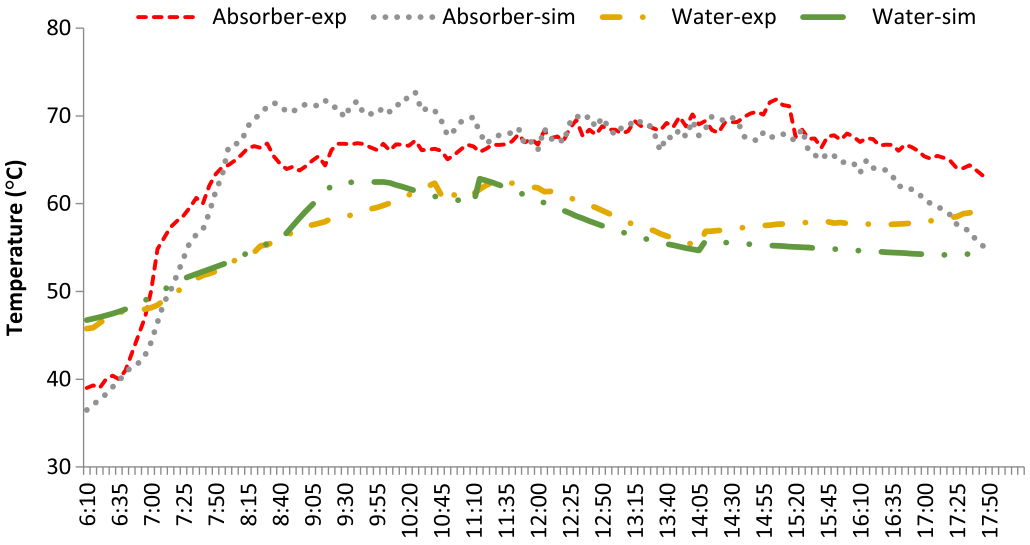

Fig. 7. The experimental and simulated temperatures of the absorber surface and water leaving the collector.

wall (90°) are compared in Figure 10. The results show that the collector installed on a sloped roof (latitude angle) performed the best, followed closely by the flat roof. The collector performance varied slightly with building type mainly due to effect of water flow rate.

3.2 Azimuth angle

The optimal orientation is determined as south facing at zero azimuth (β). However, at times, designers are required to apply collectors deviating from south that may affect Q_c

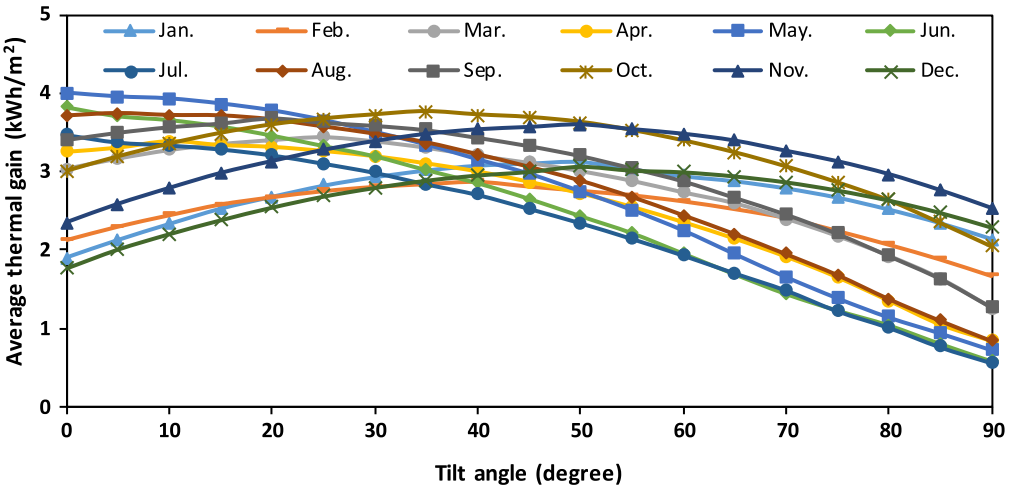

Fig. 8. Monthly average thermal energy (Q_c) produced by solar collector at various tilt angles (Φ).

Table 2. Optimum monthly collector tilt angles for enhanced thermal energy gain.

Month	Φ_{opt}	Thermal gain (Q_c)
Jan	50	3.23
Feb	40	2.97
Mar	25	3.58
Apr	10	3.59
May	0	4.11
Jun	0	3.93
Jul	0	3.57
Aug	5	3.87
Sep	20	3.81
Oct	35	3.86
Nov	50	3.72
Dec	50	3.18
Average	23.75	3.62

[28]. The impact of varying β from 90° (east) to −90° (west) with an increment of 30° was, therefore, determined on Q_c on a monthly and yearly basis as shown in Figure 11A and B. The results indicate that Qc peaked at $\beta = 0°$ for all months. An interesting observation noted that in summer months (April to August) the collector performance remained unaffected by azimuth changes while during the rest of the year (September to March) the performance decreased sharply when moving away from the south orientation. Hence, yearly Q_c of the south facing collector is 30% and 22% higher than that of west and east facing collector respectively.

3.3 Inlet flow rate

Daily water consumption for each building type is calculated per code requirements to size the collector tank and is kept fixed for the whole year. Since the collector only recovers thermal energy during the daytime, the varying daylight intensity and hours affect the amount of thermal energy available at the collector. The variable energy available at the absorber requires variable water flow rate for optimal energy recovery. The water flow rate inlet to the collector will in turn need to be optimized for different months. The total daily water demand is circulated through the collector during daytime (represented by daylight hours) at various flow rates to determine optimal flow rate for each month and building type. The summer months of May and June had the highest number of daylight hours with an average of 13 h, while the winter months of January and December had the lowest with an average of 10 h [29]. On the other hand, the heating demand naturally peaked in winter months compared to that of summer months. Additionally, each building type has different occupant loads and temperature set points which impact the optimal water flow rate for maximum thermal energy recovery. The inlet water flow rate for each of the building sector considered (residential, hospital, school, office, factories) is optimized for each month considering all the above-mentioned factors. Inlet water flow rate was found to be higher in winter months and lower in summer months yielding maximal thermal energy extraction as shown in Figure 12 while the hospital building required the highest and the most variable water flow rate.

3.4 Inlet water temperature

Since temperature of municipality supply water entering the collector is an uncontrolled parameter, its influences on the collector's performance is of interest specifically in UAE as it varies substantially among different seasons. The inlet water is assumed to be 3 to 4 °C higher than average daytime ambient temperature ($T_{avg\text{-}amb\text{-}day}$) considering the effect of ambient temperature and solar flux on the exposed storage tanks [30]. The $T_{avg\text{-}amb\text{-}day}$ in UAE was the highest in May (42 °C) and the lowest in January (26 °C) [7]. Q_c for each building type is plotted (left axis) with $T_{avg\text{-}amb\text{-}day}$ (red line on right axis) as presented in Figure 13. At the lowest $T_{avg\text{-}water\text{-}inlet}$, Q_c, is the highest

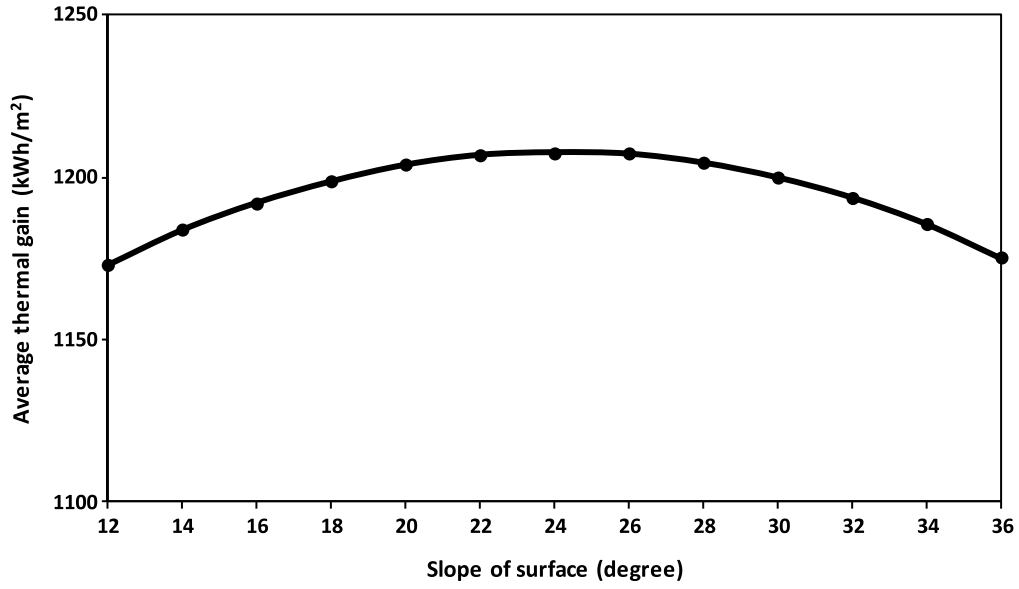

Fig. 9. Yearly thermal energy gain (Q_c) of the collector at various tilt angles (Φ) to determine energy losses at the off optimal latitude scenarios.

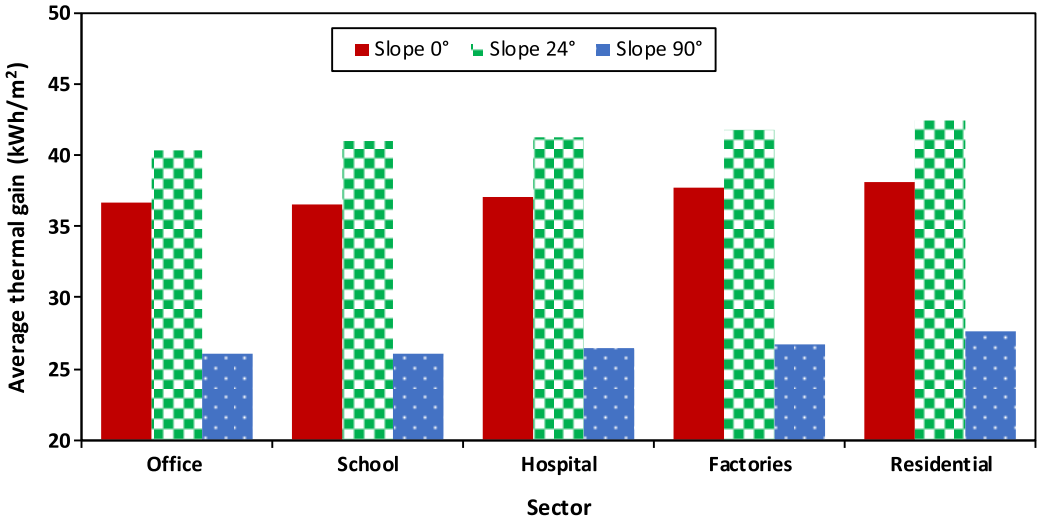

Fig. 10. Thermal energy gain (Q_c) of the collector installed at the pitched roof (24°), flat roof (0°) and vertical wall (90°).

and the vice versa which is in agreement with the collector efficiency curve shown in Figure 5. The results shown in Figure 13 confirm that the collector delivered higher thermal energy from September to April which coincides with the peak months of hot water demand. The occurrence of demand and supply peaks in the same season enabling the stakeholder to utilize maximum collector capacity.

3.5 Solar tracking

The regular building applied collectors for office, residential and commercial sectors were not tracked while tracking was considered for hospitals. However, the strong and stable radiation spanning over several daylight hours in UAE and similar contexts offers an opportunity to determine the potential enhancement in collector yield through solar tracking. The effect of solar tracking is investigated employing three tracking modes i.e., the surface rotates about a vertical axis (single-axis) to track the sun (track-1), the surface rotates about horizontal axis (single-axis) to track the latitude changes (track-2), the surface tracks in horizontal and vertical axis (double-axis) such that the beam radiation is always normal to the surface (track-3). The Q_c of tracked collector is compared with that of a static collector facing south at optimal tilt angle (24°). The net Q_c produced by collector in each tracking mode is calculated after subtracting the energy required for tracking of the collector and is presented in Figure 14. The net Q_c for track-1, track-2, and track-3 was higher than that of static collector by 5.6%, 10.3% and 13.4% respectively indicating a potential to introduce tracking option. The simulation studies are pure energy

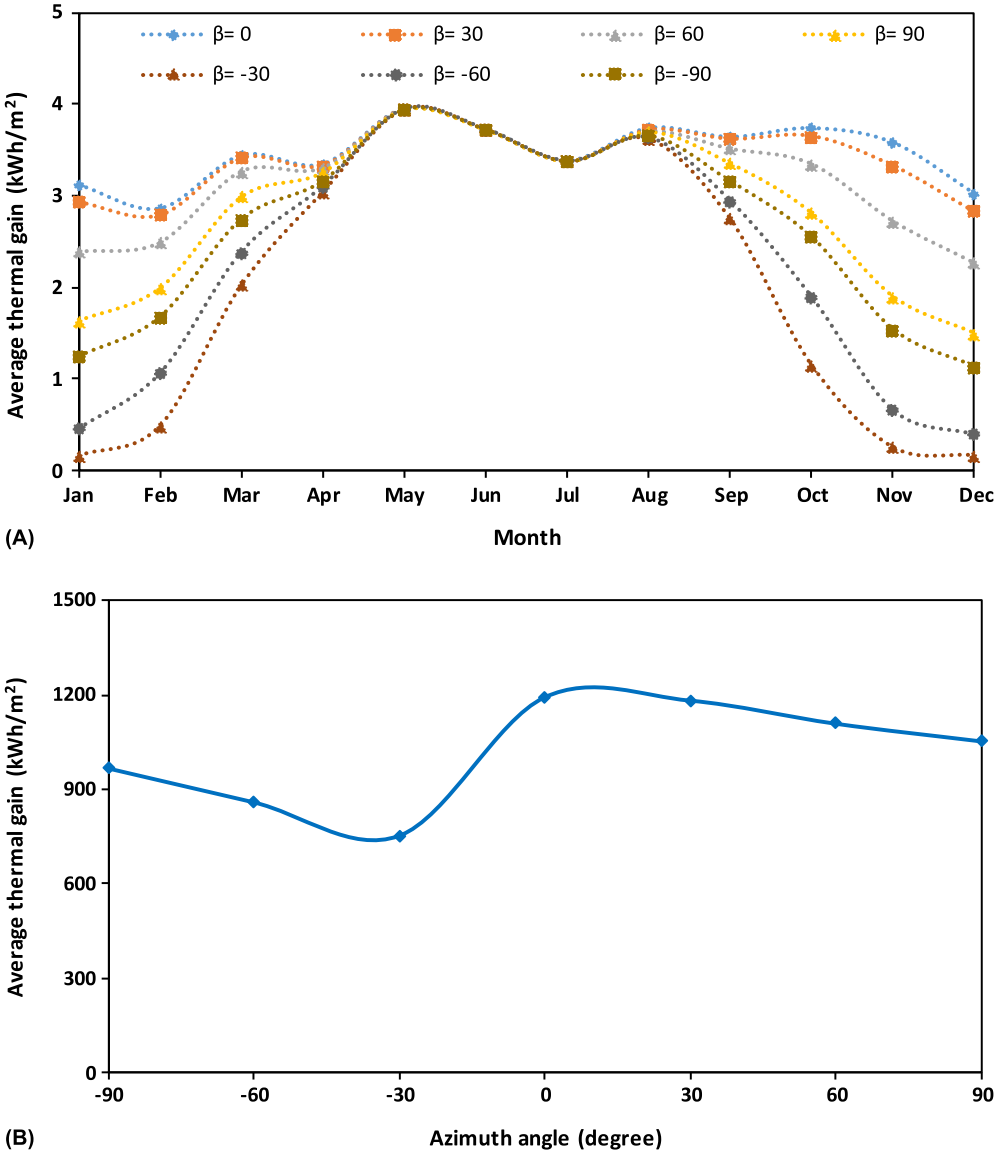

Fig. 11. (A) The impact of azimuth angle (β) on the average energy produced from the solar collector (Q_c) on average monthly basis. (B) The impact of azimuth angle (β) on the energy produced from the solar collector (Q_c) on yearly basis.

comparisons and does not include the special and structural requirements of tracking systems which needs further analysis and is out of the scope of this paper.

3.6 Solar concentration

The solar radiation as it reaches the collector surface (so called single sung) yields lower temperatures suitable for building applications that require water at 45 °C. However, for hospitals and industrial processes, the required temperatures range from 75 to 110 °C and is unlikely to be achieved by the conventional single sun collectors. To achieve such a higher temperature, modifications are required such as adding mirrors or lenses to concentrate solar radiation. The effect of solar concentration by employing geo-metrical concentration ratio (ratio of lenses or mirror area to the collector area) ranging from 1 to 5x are investigated in winter months (Dec. and Jan.) to determine their effectiveness in the worst-case scenario i.e., season of higher water demand with lower solar gains. An almost linear increase in collector outlet temperature was observed with increasing solar radiation concentration as shown in Figure 15. It was observed that without solar concentration (1x), the water temperature remained below 60 °C which can only serve domestic buildings with demand side temperature of 45 °C. The temperature required for hospital buildings (65 °C) is achieved with the concentration ratio of 2x and that required for industrial buildings (70 °C–110 °C) is achieved by concentration ratio of 3–5x. To achieve such temperatures, the collector needs modifications such as optical elements, tracking systems and structural support which involves additional space and cost which are not considered at this stage. The study therefore, is intended to determine achievable temperatures at certain concentra-

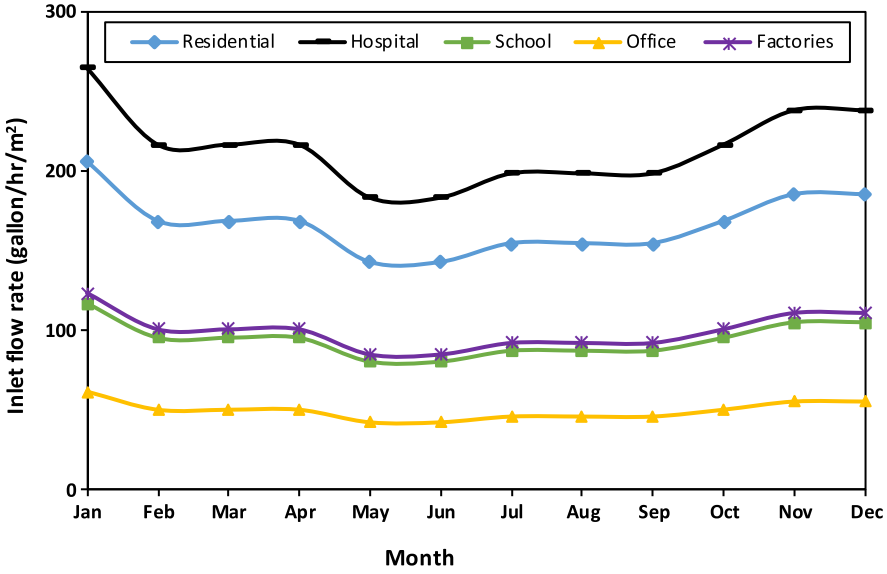

Fig. 12. Monthly average inlet water flow rate for different building type.

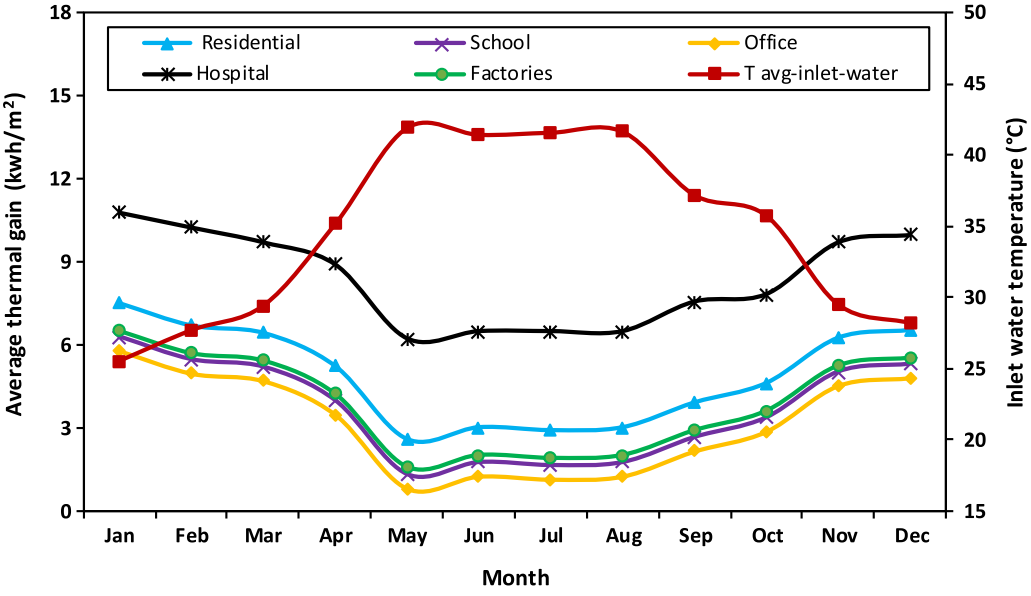

Fig. 13. Average energy contribution from the solar collector with varying inlet water temperature.

tion ratios only leaving the detailed resource input-output comparison for future studies.

4 Overall system performance

Finally, the collector is simulated using optimal collector parameters of tilt angle, azimuth angle and water flow rate discussed in previous sections to determine its effectiveness in delivering the required amount of hot water [14] and at the desired temperature [15]. The thermal energy produced by the collector is compared to the thermal energy required by each building type for the required amount of hot water production. Finally, the ratio of collector area to building foot print area is calculated to deliver the required hot water demand for each building type as shown in Table 3. The results show that the hospital building required the highest collector area per building area associated to higher occupants' density as well as hot water demand for specific activities such as equipment sterilization.

The calculated ratios should help building professionals and owners to size an optimal solar thermal collector for their respective buildings with minimal effort and yet be accurate. In design terms, however, opportunities may be sometimes limited, knowing that SWHS are traditionally installed on rooftops, the space availability may be limited due to building design (for example, in tall buildings) or the existence of other building equipment such as HVAC systems. The reported higher temperatures achieved by solar tracking and solar concentration can widen the

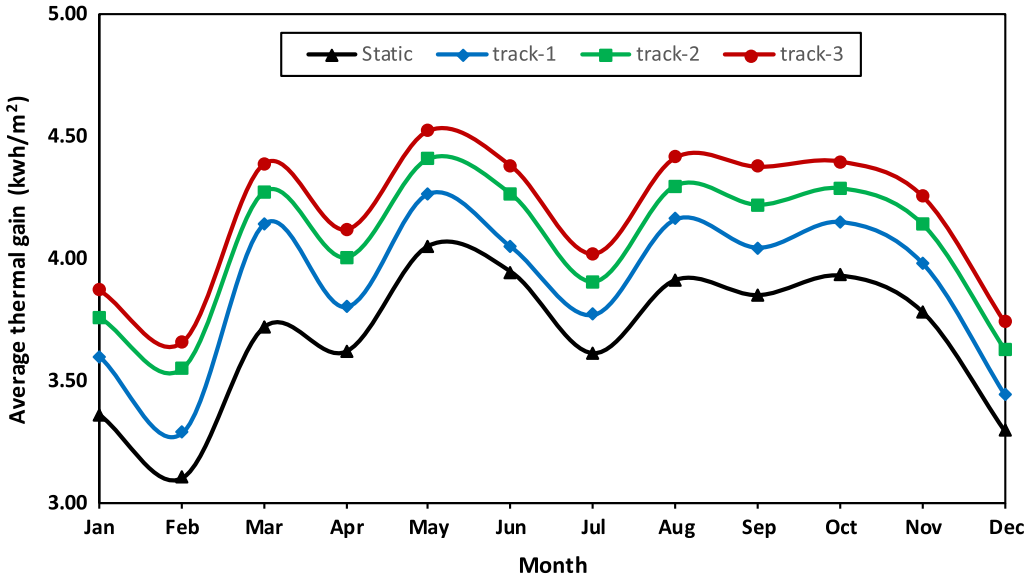

Fig. 14. Monthly average energy contribution from the solar collector with varying solar tracking modes.

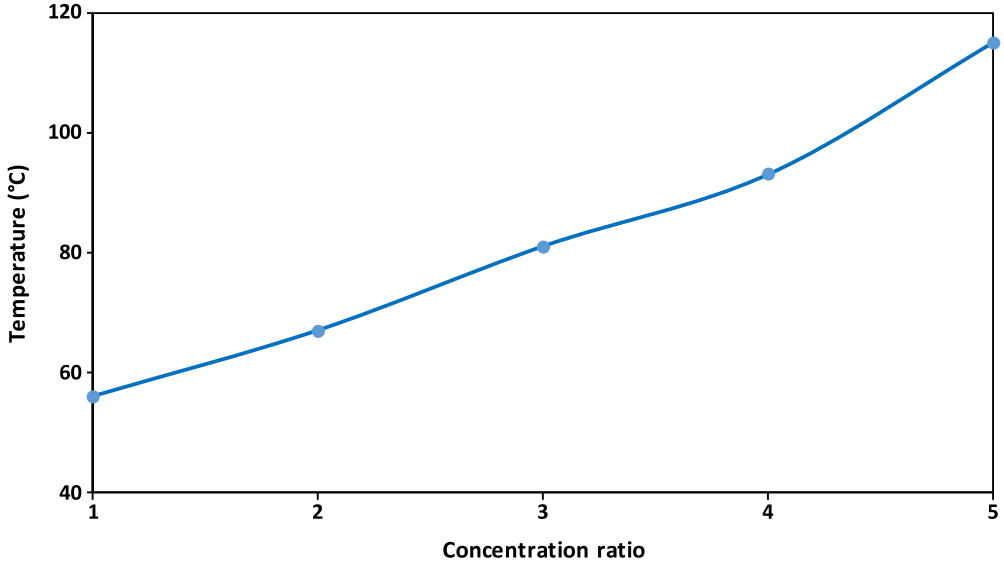

Fig. 15. Temperature variation versus solar radiation concentration.

integration of solar energy in novel areas like industries, nevertheless it comes at the expense of additional space by concentrators and tracking systems.

5 Economic analysis of the system

The economic analysis is conducted by calculating simple payback period considering the benefit of energy produced and the cost of the systems installed. The energy is converted into monetary cost and benefit by applying UAE based electricity tariff of AED 0.32/kWh [31]. To apply the electrical energy tariffs, the thermal energy is converted into equivalent electrical energy by considering a 70% depreciation in energy quality. Additional tracking, inclusive of tracking system and energy, cost is counted as $0.36 per watt installed [32] considering thermal systems equivalent of PV systems in terms of tracking. Energy consumed by the pump to circulate water through collector is calculated by assuming 10 m additional water head with a flow rate of 0.18 L/. It resulted in the additional shaft power of 30 W for pumping. The equivalent electrical energy gain for static, single axis tracked (vertical), single axis tracked (horizontal), double axis tracked, and concentrated case is 35.3 MWh/lifetime, 37.5 MWh/lifetime, 39.2 MWh/lifetime, 40.6 MWh/lifetime and 50.6 MWh/lifetime respectively. The considered costs and benefits are compiled in Table 4.

Table 3. Energy performance of the optimized solar thermal collector for various building types under different tracking options.

Sector	Parameters	Static	Single axis tracking (vertical)	Single axis tracking (horizontal)	Double axis tracking
Residential	Energy demand (MJ/day)	558	–	–	–
	Energy produced (MJ/day)	157	165	172	178
	No of collector required	7	7	6	6
	Collector area per building area	0.0142	0.0135	0.0129	0.0125
Hospital	Energy demand (MJ/day)	1470	–	–	–
	Energy produced (MJ/day)	152	161	168	173
	No of collector required	19	18	17	17
	Collector area per building area	0.0385	0.0365	0.0349	0.0340
School	Energy demand (MJ/day)	315	–	–	–
	Energy produced (MJ/day)	151	160	167	172
	No of collector required	4	4	4	3
	Collector area per building area	0.0083	0.0079	0.0075	0.0073
Office	Energy demand (MJ/day)	166	–	–	–
	Energy produced (MJ/day)	68	72	75	77
	No of collector required	5	5	4	4
	Collector area per building area	0.0098	0.0093	0.0089	0.0086
Factories	Energy demand (MJ/day)	949	–	–	–
	Energy produced (MJ/day)	154	163	170	175
	No of collector required	12	12	11	11
	Collector area per building area	0.0245	0.0232	0.0222	0.0216

Table 4. Cost estimation of the set-ups and their monetary benefits.

Cost ($)	Static FPC	Tracked FPC	Concentrated FPC
Collector cost	756	756	756
Pump cost	50	50	50
Tracking cost	0	36	36
Concentrator cost	0	0	125
Pumping energy cost	108	108	108
Tracking energy cost	0	36	0
Total cost ($)	914	950	1039

	Thermal energy (kWh/day)	Equivalent electrical energy (kWh/day)	Yearly electrical energy (MWh/year)	Yearly saving ($)
Static	39.2	11.76	3.5	304
Single axis tracking (vertical)	41.7	12.51	3.7	322
Single axis tracking (horizontal)	43.6	13.08	3.9	340
Double axis tracking	45.1	13.51	4.1	357
Concentrator	56.2	16.86	5.1	444

The simple payback period is calculated by dividing the total cost of the system (initial investment as well as operating cost) by the economic benefit of the energy produced in the first year applying the values of energy harvested and electricity rates. The static case has the longest payback period of almost 3 years. Payback period reduced gradually with the improvement in thermal gain via different ways of tracking and/or concentration. In the optimized case, the payback period is reduced to almost 2 years.

6 Conclusion

This study examined the energy performance of SWHS in various building types under the hot climate of UAE, through TRNSYS simulation model. The parametric simulation determined the optimal collector parameters of tilt angle, azimuth angle and collector inlet water flow rate with respect to different seasons, building types and water demands. An optimal tilt angle of each month was identified to exploit the maximum potential of the system in Abu Dhabi, UAE which ranged from 50° at maximum for January to 0° for May. The optimum azimuth angle was found to be 0° (south facing) rendering a drop of 22% and 30% in thermal yield when the collector faced exact East and West respectively. It was observed that the roof applied collectors (both flat and pitched) are more effective than wall mounted collectors. Eventually, the collector area required per building area was determined for each building type with the hospital requiring, in the best case, the highest ratio value. The solar collector tracking was then evaluated as a means of reducing the area allocated to install the collectors on top of a roof or on a facade. The needs for solar radiation concentration is determined for some building types to deliver the higher required temperatures. It was also evident that the number of required collectors decrease for each building as the axis of tracking increases. Finally, the system feasibility is calculated for the payback period and the optimized case will be able to return its cost in almost 2 years.

These results would provide building professionals with a quick assessment of the possibility to integrate the required area or number of SWHS collectors to meet the hot water demand in new or retrofitted buildings.

Nomenclature

A_c	aperture area of the collector (m^2)
C_{HX}	heat-capacitance of coiled heat-exchanger (kJ/K)
C_{pc}	specific heat of collector fluid (kJ/(kg K))
C_{tank}	heat capacitance of storage tank (kJ/K)
DHW	domestic hot water
f_c	collector-fin efficiency factor
f_r	overall collector heat-removal efficiency factor
I_b	incident-beam radiation per unit area (kWh/m^2)
I_d	diffused radiation per unit area (kWh/m^2)
I_t	global radiation on horizontal surface per unit area (kWh/m^2)
I_{ti}	total incident-radiation on a flat surface per unit area (kWh/m^2)
m_c	collector fluid mass-flow rate (kg/h)
n_c	number of collectors mounted in series
n_g	number of glass covers
Q_c	rate of heat gain collector array (kW)
$Q_{\text{in, HX}}$	rate of heat gains of coiled heat-exchanger (kW)
$Q_{\text{in, tank}}$	rate of heat gains of storage tank (kW)
$Q_{\text{out, HX}}$	rate of heat loss of coiled heat-exchanger (kW)
$Q_{\text{out, tank}}$	rate of heat loss from storage tank (kW)
r_g	ground reflectance
SWHS	solar water heating systems
SHC	solar heating and cooling systems
T_a	ambient temperature (°C)
T_{av}	collector-fluids average temperature (°C)
T_{hwa}	hot-water average temperature (°C)
T_{hw1}	hot-water initial temperature (°C)
T_{hw2}	hot-water final temperature (°C)
T_{HX}	temperature of coiled heat-exchanger (°C)
T_i	temperature of fluid entering the collector (°C)
T_p	collector-plates temperature at stagnation (°C)
T_{tank}	temperature of storage tank (°C)
U_{be}	heat loss coefficient of collector bottom surface (kWh/m^2K)
U_c	overall heat loss-coefficient of collector (kWh/m^2K)

Symbols

α	absorptance of absorber plate
ε_g	emissivity of glass covers
ε_p	emissivity of absorber plate
σ	Stefan–Boltzmann constant ($5.6697 \times 10^{-8}\,W/(m^2K^4)$)
τ	transmittance of absorber plate
Δt	simulation time-step (h)
φ	collector latitude angle (°)
β	collector azimuth angle (°)
Φ	collector tilt angle (°)

The authors gratefully acknowledge financial support from the United Arab Emirates University through the Emirates Centre for Energy and Environment research funded project (31R054).

References

1. Dubai Electricity & Water Authority (DEWA), Annual Statistics, https://www.dewa.gov.ae/en/about-dewa/about-us/dewa-publications/annual-statistics
2. U.S. Environmental protection agency, draft inventory of U. S. greenhouse gas emissions and sinks:1990–2014 (U.S. environmental protection agency, Washington, 2016)
3. U.S. Energy information administration, issues in international energy consumption analysis: Canadian energy demand, (2015)

4. R. Kempener, G. Simbolotti, G. Tosato, *Solar Heating and Cooling for Residential Applications* (International renewable energy agency, 2015)
5. M.D. Islam, I. Kubo, M. Ohadi, A.A. Alili, Measurement of solar energy radiation in Abu Dhabi, UAE, Appl. Energy **86**, 511–515 (2009)
6. A. Hasan, H. Alnoman, Y. Rashid, Impact of integrated photovoltaic-phase change material system on building energy efficiency in hot climate, Energy Build. **130**, 495–505 (2016)
7. A. Hasan, K.A. Al-Sallal, H. Alnoman, Y. Rashid, S. Abdelbaqi, Effect of Phase Change Materials (PCMs) Integrated into a Concrete Block on Heat Gain Prevention in a Hot Climate, Sustainability **8**, 1009 (2016)
8. F.A. Ghaith, R. Abusitta, Energy analyses of an integrated solar powered heating and cooling systems in UAE, Energy Build. **70**, 117–126 (2014)
9. A. Al-Alili, M.D. Islam, I. Kubo, Y. Hwang, R. Radermacher, Modeling of a solar powered absorption cycle for Abu Dhabi, Appl. Energy **93**, 160–167 (2012)
10. F. Jafarkazemi, S.A. Saadabadi, Optimum tilt angle and orientation of solar surfaces in Abu Dhabi, UAE, Renew. Energy **56**, 44–49 (2013)
11. A. Khalil, A. Alnajjar, Experimental and theoretical investigation of global and diffuse solar radiation in the United Arab Emirates, Renew. Energy **6**, 537–543 (1995)
12. A transient system simulation program-program manual, University of Wisconsin-Madison, USA: Solar energy laboratory, TRNSYS 17 (2004)
13. International Building Code 2009, https://law.resource.org/pub/us/code/ibr/icc.ibc.2009.html
14. ASHRAE HANDBOOK 2011 HVAC Applications SI Edition
15. The engineering toolbox (2016), http://www.engineeringtoolbox.com/design-hot-water-system-d_92.html
16. S.A. Klein, Calculation of flat-plate collector loss coefficients, Sol. Energy **17**, 79–80 (1975)
17. Solar-energy laboratory, IIsibat version 3.0.0.26, TRNSYS 15.3., Solar-energy laboratory university of Wisconsin Madison
18. M.R. Islam, K. Sumathy, S.U. Khan, Solar water heating systems and their market trends, Renew. Sustain. Energy Rev. **17**, 1–25 (2013)
19. I.R. Pillai, R. Banerjee, Impact of hot water usage pattern and location on economics of solar water heating systems, Water Energy Abstr. 14, (2004)
20. A. Lowenstein, C. C. Hiller, Disaggregating residential hot water use – Part II', ASHRAE Trans. **104**, 1852–1863 (1998)
21. NAHB Research Center, Inc (2002), Performance comparison of residential hot water systems, Report prepared for National Renewable Energy Laboratory, Colorado
22. A. Gadgil, Economic, materials and performance constraints on the design of a solar DHW system for use in India, SESI J. **1**, 31–36 (1987)
23. I.R. Pillai, R. Banerjee, Methodology for estimation of potential for solar water heating in a target area, Sol. Energy 81, 162–172 (2007)
24. K. L. Narkhede, Solar water heater as a demand side management option, M. Tech. Dissertation, Energy Systems Engineering, (Indian Institute of Technology, Bombay, India, 2001)
25. A. Shariah, M.A. Al-Akhras, I.A. Al-Omari, Optimizing the tilt angle of solar collectors, Renew. Energy **26**, 587–598 (2002)
26. H. Moghadam, F.F. Tabrizi, A.Z. Sharak, Optimization of solar flat collector inclination, Desalination **265**, 107–111 (2011)
27. M.D. Islam, A.A. Alili, I. Kubo, M. Ohadi, Measurement of solar-energy (direct beam radiation) in Abu Dhabi, UAE, Renew. Energy **35**, 515–519 (2010)
28. M. Kacira, M. Simsek, Y. Babur, S. Demirkol, Determining optimum tilt angles and orientations of photovoltaic panels in Sanliurfa, Turkey, Renew. Energy **29**, 1265–1275 (2004)
29. L. El Chaar, L.A. Lamont, Global solar radiation: multiple on-site assessments in Abu Dhabi, UAE, Renew. Energy **35**, 1596–1601 (2010)
30. A. Hasan, H. Alnoman, A.H. Shah, Energy efficiency enhancement of photovoltaics by phase change materials through thermal energy recovery, Energies **9**, 782 (2016)
31. Dubai Electricity & Water Authority – tariff, https://www.dewa.gov.ae/en/customer/services/consumption-services/tariff
32. Solar Balance-of-System: To Track or Not to Track, Part I, https://www.greentechmedia.com/articles/read/solar-balance-of-system-to-track-or-not-to-track-part-i

Cite this article as: K. Tabet Aoul, A. Hasan and H. Riaz: Solar water heating systems for different buildings under a hot climate; parametric optimization and economic analysis. Sust. Build. **3**, 3 (2018).